Predominance of multielectron processes contributing to the intrinsic spectra of low-energy Auger transitions in copper and gold

S. F. Mukherjee, K. Shastry, and A. H. Weiss
Department of Physics, University of Texas at Arlington, Arlington, Texas 76019, USA
(Received 17 June 2011; revised manuscript received 4 September 2011; published 12 October 2011)

Positron-annihilation-induced Auger electron spectroscopy (PAES) was used to obtain Cu and Au Auger spectra that are free of primary-beam-induced backgrounds by impinging the positrons at an energy below the secondary-electron-emission threshold. The removal of the core electron via annihilation in the PAES process resulted in the elimination of postcollision effects. The spectra indicate that there is an intense low-energy tail (LET) associated with the Auger peak that extends all the way to 0 eV. The LET is interpreted as indicative of processes in which filling of the core hole by a valence electron results in the ejection of two or more valence electrons which share the energy of the conventional core-valence-valence Auger electron.

DOI: 10.1103/PhysRevB.84.155109 PACS number(s): 78.70.Bj, 82.80.Pv, 68.49.−h, 79.20.Hx

I. INTRODUCTION

Electron and x-ray-induced Auger electron spectroscopy (EAES and XAES) are sensitive to the composition and chemistry of the topmost layers of a surface[1–3] owing to the short inelastic mean-free path of electrons (5–20 Å) emitted in the Auger energy range (∼20–2000 eV).[4,5] However, the surface-related spectral contributions in EAES and XAES are accompanied by a large background which leads to uncertainty in the determination of Auger line shapes and in the quantitative analysis of Auger spectra. This background cannot be avoided due to the fact that the incident electron or photon beam energy must exceed the ionization energy required to create the core hole that gives rise to the Auger transition. Secondary-electron cascade processes due to the scattering of the incident electron beam (in the case of EAES) or the scattering of photoexcited valence and core electrons (in the case of XAES) result in a background signal. This background in EAES extends from the low-energy secondary-electron peak to the incident-beam energy and, consequently, to energies in the range of the Auger peaks. In addition, incident beams with keV energies cause Auger excitations many inelastic mean-free paths below the surface. Consequently, EAES has a large extrinsic background under the Auger peaks due to the primary beam and even larger extrinsic backgrounds under the low-energy portion ($\leqslant 10^2$ eV) of the Auger electron spectrum due to both beam-induced secondaries and contributions from Auger electrons that lose energy as they exit from atoms excited deep below the surface. Although sophisticated methods have been developed to remove the large backgrounds with XAES and EAES (see, for instance, Ref. 6, and references therein), the fact that the extrinsic background under the low-energy Auger lines ($\leqslant 10^2$ eV) is many times larger than the Auger signal makes it impossible to obtain a model-free determination of the Auger line shape.

Previous studies[7,8] have shown that low-energy positrons can induce Auger electron emission selectively from the topmost atomic layer of surfaces as a result of the annihilation of the surface-trapped positrons with core electrons. Recently, Mukherjee *et al.* have shown that it is possible to efficiently excite Auger transitions by trapping positrons directly into these surface states using a low positron beam energy (∼1.5 eV) which is well below the threshold for secondary-electron emission.[9] Here, we report measurements exploiting this effect to measure the energy spectrum of electrons resulting from Auger transition in the top layer of Au and Cu crystals that are completely free of extrinsic beam-induced secondary electrons. Additionally, such PAES spectra are free of postcollision interaction (PCI) effects as the initial core electron is annihilated to initiate the Auger process (refer to Fig. 1). The measured spectra therefore consist exclusively of electrons emitted as a direct result of the Auger transition itself (CVV) and electrons emitted via intrinsic loss processes (e.g., C-VVV transitions, etc.)[1] (C, core; V, valence).

The spectral intensity on the low-energy side of the Auger peak, referred to as low-energy tail (LET), has been studied earlier by Auger-photoelectron coincidence spectroscopy (APECS)[10–12] and PAES.[13] The APECS studies were inconclusive as they were limited in the energy range studied (30–70 eV) and the fact that the signal was an average over several atomic layers. The APECS spectra were further limited due to the background resulting from true coincidences involving inelastically scattered photoelectrons from the valence band. Earlier PAES experiments employed a positron beam of ∼18 eV and hence the lowest-energy part of such spectra ($\leqslant$15 eV) were dominated by extrinsic electrons excited directly as a result of collisions with the incident positrons. The data reported in this paper constitute the first spectra measured with positron energy below the secondary-electron threshold and thus free of beam-induced extrinsic secondaries all the way down to 0 eV.

By eliminating the large extrinsic contributions at low energy ($\leqslant$100 eV), we have been able to show conclusively that there is a low-energy tail (LET)[10] with intensity (I_{LET}) ∼ 3.74 (3.43) times that of the Auger peak intensity (I_{peak}) for Cu (Au) at energies below the Auger energy and extending to 0 eV. The LET has been interpreted as arising mostly from intrinsic loss associated with the creation of the core hole. The spectral weight of the intrinsic part of the LET is 1.81 (2.0) times that of the Auger peak area, which is considered evidence of multielectron emission once the core hole is created. This process is analogous to the double-Auger process in noble gases[14] and similar to photon-induced correlated electron emission from solids.[15] The results have been interpreted as signature of electron correlation in the valence band.[10,12]

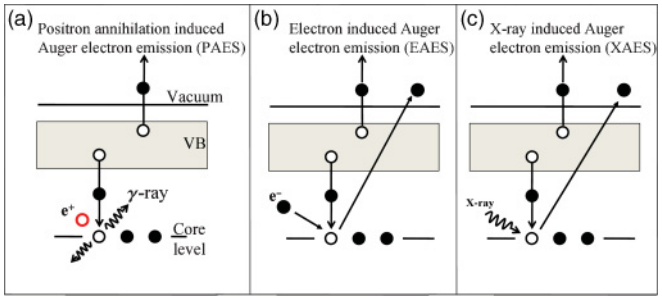

FIG. 1. (Color online) Energy-band diagram showing mechanism for (a) PAES, (b) EAES, and (c) XAES. In PAES, the core hole is created by matter-antimatter annihilation and hence it is possible to get Auger emission with incident positron energy $E_p \rightarrow 0$ eV. As opposed to EAES and XAES, the postcollision interaction (PCI) effects are absent in PAES since the core electron is annihilated.

II. EXPERIMENTAL

The experiments were carried out in the time-of-flight positron-annihilation-induced Auger electron spectrometer (TOF-PAES)[16] which uses a magnetic bottle analyzer.[17] Positrons emitted via beta decay from a 4 mCi ^{22}Na source were moderated using polycrystalline tungsten (W). The upper limit on the positron beam energy, E_p, is given by the following equation:

$$E_p = \varphi_m^+ + e(V_m - V_s), \tag{1}$$

where φ_m^+ is the positron work function of the moderator (2.9 eV), V_m and V_s are the bias on the moderator and sample with respect to the ground, respectively, and e is the electronic charge. The low-energy positrons are guided to the sample, located 3.5 m away, using an axial magnetic field. The whole spectrometer was housed in Helmholtz coils which were used to cancel out the Earth's magnetic field.

The incident beam profile [shown in Fig. 2(b)] at 0 eV sample bias was fitted with a Gaussian of 0.4 eV full width at half maximum (FWHM) and maximum at 0.65 eV. 99% of the positrons have energy less than 1 eV and this is referred to as the beam energy. This beam energy was used to obtain the Auger spectra of Cu and Au. During the measurements of the Auger spectra, the sample was biased at −0.5 V with respect to the TOF drift tube.

The annihilation gamma rays are detected by BaF_2 and NaI detectors as shown in Fig. 2(a). The outgoing electrons from the sample are parallelized using the divergent field of a permanent magnet. The electrons then travel down a retarding TOF tube and are detected by a microchannel plate (MCP). The MCP signal is used as the START signal, while the delayed BaF_2 signal provides the STOP (reverse timing) signal of the time to amplitude convertor (TAC). The TOF-PAES spectra are obtained by histogramming the output of the TAC. A calibration procedure (detailed in Ref. 9) was used to determine the relation between the measured time of flight and the kinetic energy of the electrons (referenced to the vacuum level) leaving the sample.

To estimate the contribution of accidental coincidences to TOF-PAES spectra, a second setup referred to as the triple-coincidence setup was used which takes advantage of the fact that the annihilating gamma rays are emitted at an angle of

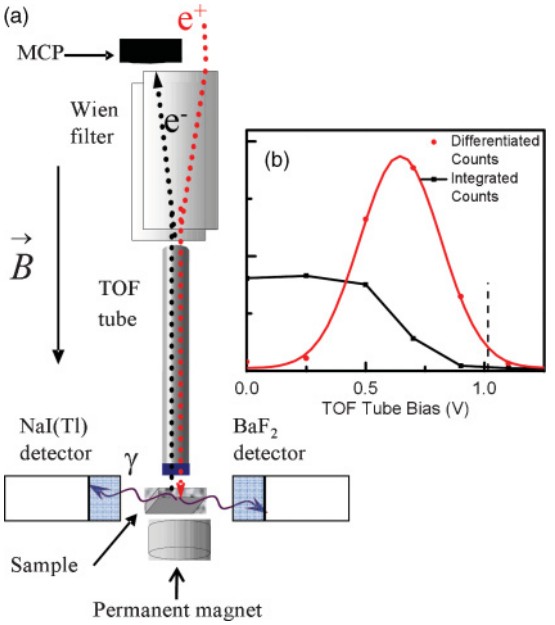

FIG. 2. (Color online) Experimental setup for time-of-flight positron-annihilation-induced Auger electron spectroscopy (TOF-PAES). (a) Schematic of the spectrometer. (b) The incident positron beam energy used to obtain the Auger spectra. The dashed line (1 eV) refers to the incident positron energy and 99% of positrons have energy less than this value (e^+, positrons; e^-, electrons; and B, magnetic field).

∼180° with respect to each other. In this setup, the STOP signal is the coincidence detection of the collinear 511 keV gamma rays by BaF_2 and NaI(Tl) [see Fig. 2(a)]. The triple-coincidence setup, by requiring the detection of two almost antiparallel gamma rays, was designed to discriminate against events in which one or both of the annihilation gamma rays generate secondary electrons as a result of Compton scattering in the sample or surrounding chamber walls.

The 4 mT transport field used in the TOF-PAES is particularly well suited for the efficient transport of the low-energy positron to the sample (which was incident at 1.5 eV at the sample) as well as the transport of the low-energy electrons emitted from the sample. A negative sample bias was used to boost the kinetic energy of electrons emitted from the surface permitting measurements of electrons emitted from the surface all the way down to 0 eV. To test the sensitivity of the TOF spectrometer to low-energy electrons, the positron beam energy was increased to just above the secondary-electron-emission threshold (∼2 eV) (Ref. 9) [refer to Eq. (1)], allowing us to observe a low-energy secondary-electron peak at ∼1 eV in addition to the Auger peak (see Fig. 3). The peaks in the timing spectra (Fig. 3) are the Auger peak and the positron sticking-induced secondary-electron peak.[9] The lagging edge of the secondary-electron peak (corresponding to the longest flight times) moves to a higher flight time as the sample bias is changed from −1 V [Fig. 3(a)] to −0.5 V [Fig. 3(b)]. These results confirm the ability of the TOF-PAES system to detect and measure the energy of electrons emitted from the sample down to sub-eV energies. To obtain the Auger spectra, the beam energy was changed back to a 1 eV beam incident on the sample at 0 V bias. All the Auger spectra were

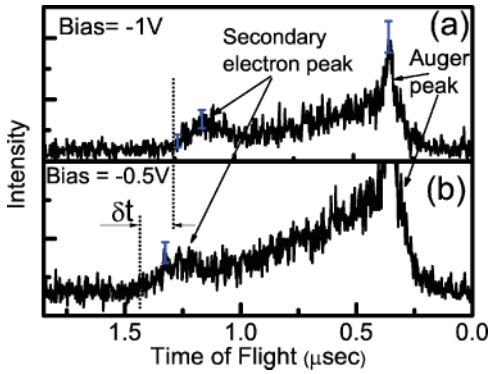

FIG. 3. (Color online) PAES spectra from Au obtained with a bias of −1 and −0.5 V. The spectra contain a sticking-induced secondary-electron peak (Ref. 9) and an Auger peak. The incident positron beam energy at 0 V sample bias is 2 eV. The flat background corresponds to accidental coincidences. The vertical dotted line in both panels shows the lagging edge of the secondary-electron peak which corresponds to electrons leaving the sample with zero kinetic energy just outside the surface. The lagging edge shifts to higher flight times as the sample bias is changed from −1 to −0.5 V, demonstrating that our spectrometer is capable of detecting electrons with energies greater than 0.5 eV.

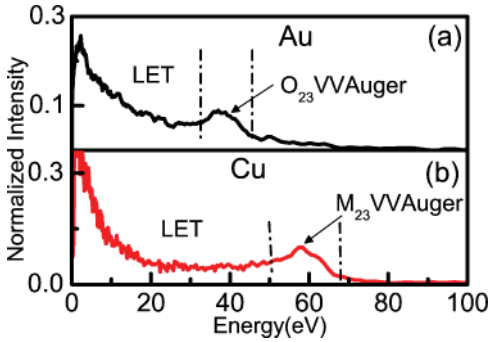

FIG. 4. (Color online) PAES spectra of (a) Au ($O_{23}VV$) and (b) Cu ($M_{23}VV$) obtained using a positron beam with kinetic energy of 1.5 eV at the sample. The energy scale represents the kinetic energy of the electrons leaving the surface of the sample. The region enclosed by dashed lines indicates the CVV Auger transition, while the intensity on the left side is the low-energy tail.

taken with this energy setting and a sample bias of −0.5 V. The time of flight for a 0.5 eV electron (corresponding to 0 eV kinetic energy emission from the sample) was ∼2 μs, which was well within the measuring range of the spectrometer.

The Au sample (a 99.985% pure polycrystalline foil, 0.025 mm thickness) was sputter cleaned every 12 h, whereas the Cu(100) sample (a 99.9% pure, 10 mm diameter × 1 mm thickness) was sputter cleaned followed by annealing at 740 °C every 12 h. While taking data the chamber pressure was maintained at 7×10^{-10} Torr. The PAES spectrum was used to monitor the cleanliness of the samples. No significant surface contamination was observed in the period between the two sputtering times. Based on oxidation studies of Ref. 18, we estimate oxygen contamination to be less than 1%.

III. RESULTS AND DISCUSSION

The PAES spectra with Cu $M_{23}VV$ and Au $O_{23}VV$ Auger peaks are shown in Fig. 4. The LET can be seen to extend from 0–50 eV for Cu and 0–30 eV for Au. Our data indicate that the LET is too intense to be accounted for by inelastic scattering of the Auger electrons from the surface. The argument that the LET is due to the Auger electrons only can be ruled out by noting that secondary-electron yield (δ) will be ∼3.73 (3.4) for Cu (Au), while the maximum value of δ for most metals is 1.8.[19] We did not observe any prominent plasmon peaks on the low-energy side of the Auger peak, which is consistent with other PAES studies.[13,20]

Following the argument of Refs. 10 and 11, the LET intensity associated with the Auger peak can be broken into intrinsic and extrinsic contributions

$$I_{\mathrm{LET}}(E) = I_{\mathrm{LET}}^{\mathrm{intrinsic}}(E) + I_{\mathrm{LET}}^{\mathrm{extrinsic}}(E), \tag{2}$$

where $I_{\mathrm{LET}}(E)$ is the spectrum in the LET region and the terms on the right side of the equation are the intrinsic and extrinsic contributions, respectively. The extrinsic part, in a usual EAES spectrum, is caused by the primary beam and the transport of Auger electrons through the solid. As suggested in Refs. 21 and 22, the extrinsic part can have two components:

$$I_{\mathrm{LET}}^{\mathrm{extrinsic}}(E) = BI(E) + I_{\mathrm{Auger}}^{\mathrm{extrinsic}}(E), \tag{3}$$

where $BI(E)$ is the primary-beam-induced secondary-electron spectrum and $I_{\mathrm{Auger}}^{\mathrm{extrinsic}}(E)$ is the spectrum due to inelastic scattering of the Auger electrons with surface and subsurface atoms.[21] The area under the Auger peak in each PAES spectrum (50–70 eV for Cu and 30–50 eV for Au) is referred to as I_{peak}. The inherent assumption in these analyses is that the creation of true Auger electrons (CVV) and their subsequent transport and emission can be treated separately.[23]

As discussed above, we used an incident beam whose energy was below the secondary-electron-emission threshold. It has been demonstrated in Ref. 9 that the threshold for positron-induced secondary-electron emission is given by

$$E_{K\,\max} = E_p - \varphi^- + E_b, \tag{4}$$

where $E_{K\,\max}$ is the maximum energy of emitted electrons, φ^- is the electron work function, and E_b is the binding energy of the positron in the image potential well.[9] For Cu(Au), $\varphi^- = 4.6(5)$ eV (Ref. 24) and $E_b = 2.7(2.9)$ eV, and hence the threshold for secondary-electron emission is ∼2 eV. The Auger spectra shown in Fig. 4 were obtained with an incident beam whose kinetic energy on the sample surface was 1.5 eV, thus making the beam-induced secondary-electron-emission channel energetically forbidden [$BI(E) = 0$].

Earlier studies[25] have shown that background due to positron-annihilation-gamma-ray-induced secondary electrons is not significant in the PAES measurements. These experiments showed that it was possible to turn off the positron-annihilation-induced Auger signal by thermally desorbing the positrons from the surface state into the vacuum as positronium (Ps, a hydrogenlike atom composed of an electron and positron). Most of the Ps annihilate in close proximity to the sample. Consequently, if gamma-ray-induced secondary electrons were a significant source of background signal, that signal should still be present even after the positrons are desorbed from the surface state as Ps. The data in Fig. 5(a)

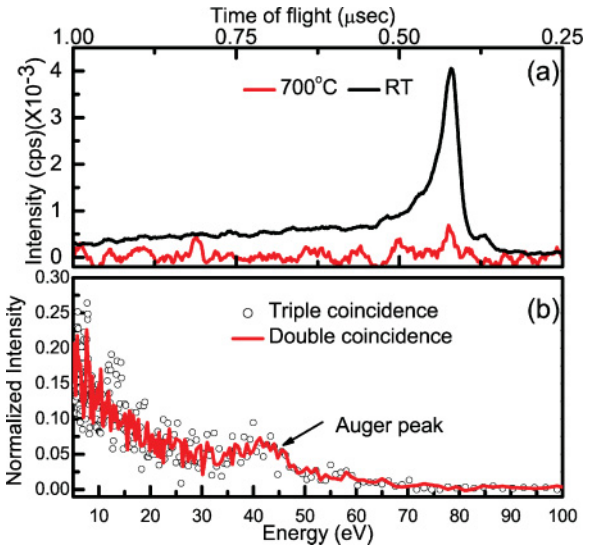

FIG. 5. (Color online) Estimation of gamma-induced secondary-electron contribution to LET. (a) Comparison of PAES spectrum of Cu obtained at room temperature (RT) and at 700 °C. (b) Normalized PAES and triple-coincidence spectra from Au surface. The triple-coincidence setup is biased against the gamma-ray-induced background.

show the results of experiments, which are similar to those of Ref. 25. The average count rate of the high-temperature spectrum (700 °C) is only ∼2% of the room temperature (RT) count rates (obtained after cooling the sample to room temperature). This result provides an upper bound on the gamma-induced secondary background (∼2% of the observed LET) and demonstrates that such secondaries are not an important source of background in our measurements.

Further verification of the absence of this channel is obtained by comparing the PAES signal to the triple-coincidence setup described above. In the latter, a measured coincidence between the two annihilation gamma rays, emitted at an ∼180° angle to each other, was required in order to produce a valid STOP signal to the TAC. The triple-coincidence measurement insured that the annihilation events were taking place at the sample since two gamma annihilations taking place at some distance from the sample would not be in the simultaneous view of both detectors. The requirement of triple coincidence would strongly suppress background due to (i) annihilation-induced secondary electrons generated on surfaces other than the sample, and (ii) events where one of the gamma rays undergoes Compton scattering or photoemission in the sample. The PAES and the triple-coincidence spectrum from Au are shown in Fig. 5(b). The LET region (0 − 30 eV) can be seen to have similar intensity in both the PAES and triple-coincidence spectra (the poorer statistics of the triple-coincidence measurements are a consequence of the low count rates associated with the reduced joint detection efficiency of the two gamma detectors), proving that the gamma-induced background has negligible contribution to the LET.

Next, the extrinsic contribution to the LET by the Auger electrons undergoing scattering in the surface and subsurface region is explored. Assuming isotropic emission, half of the Auger electrons are emitted toward the subsurface region, while the other half is emitted toward the surface and vacuum (forward direction). Few of the Auger electrons emitted toward the subsurface will elastically backscatter [given by ratio R (Ref. 26)] and will contribute to the Auger peak. Of the forward-emitted electrons, some will make it to the detector without suffering any inelastic collision giving rise to the Auger peak. The ratio of these Auger electrons (no inelastic collision) to all the electrons emitted in the forward direction is given by the transmission factor, T, which can be calculated using the Beer-Lambert cosine law[27]

$$T = \frac{\int_0^{2\pi} d\phi \int_0^{\pi/2} \exp\left(\frac{-d}{\lambda_{\mathrm{EAL}}^{\mathrm{Cu,Au}} \cos\theta}\right) \sin\theta \, d\theta}{\int_0^{2\pi} d\phi \int_0^{\pi/2} \sin\theta \, d\theta}, \qquad (5)$$

where $\lambda_{\mathrm{EAL}}^{\mathrm{Cu,Au}}$ is the effective attenuation length[28–31] of the Auger electron from Cu(Au), d is the distance the electrons travel in the solid (1.28 Å), θ is the angle from the surface normal, and ϕ is the azimuthal angle. Hence, $T =$ 46% (47%) has been calculated for Cu M_{23}VV (Au O_{23}VV) Auger electrons. Thus a number of Auger electrons, given by $I_{\mathrm{peak}}[(1-T)/(T+R)]$, will inelastically scatter in the selvedge layer and contribute to the extrinsic electrons in the PAES spectra. To understand their contribution, we took PAES spectra from a Cu surface with different coverages of residual gases, as shown in Fig. 6. It can be noticed that the major affect of altering the surface roughness or chemistry is in the low-energy part of the LET (<30 eV for Cu). Thus we conclude that the Auger-electron scattering from the selvedge layer contributes mostly to the cascade region of the LET. The secondary-electron yield due to these electrons is referred to as $\delta_{\mathrm{surface}}$.

For the electrons which are emitted toward the subsurface region, they can be thought of as a beam of electrons incident on the sample from outside. Hence it is reasonable to assume that their contribution will be restricted to the cascade region. The number of such electrons can be easily shown to be $I_{\mathrm{peak}}[(1-R)/(T+R)]$ and their secondary-electron yield is referred to as δ_{bulk}.

The secondary-electron spectrum produced by inelastic scattering of the Auger electrons with the surface and the subsurface region has been modeled as suggested by Ref. 33 and is expressed as $I(E) \sim E(E+E_{\mathrm{PB}})^{-1}(E+\varphi^{-})^{-m}$, where $I(E)$

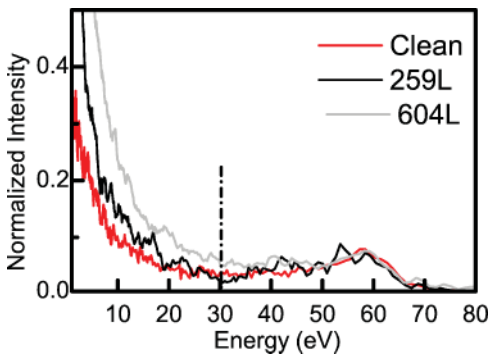

FIG. 6. (Color online) Normalized Cu-PAES spectra with different coverages of residual gas. As can be seen, the effect of surface scattering is mostly in the cascade region (<30 eV). A similar trend can be observed in Ref. 32.

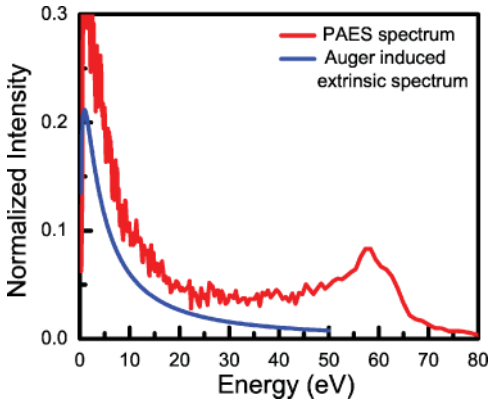

FIG. 7. (Color online) Estimate of the extrinsic background due to Auger-electron scattering in the surface and subsurface region from Cu surface. The normalized Auger-electron-induced extrinsic spectrum (as suggested by Ref. 33) is compared to the PAES spectrum.

is the intensity of the secondary-electron spectrum, E is the electron energy, E_{PB} is the energy of the primary beam, φ^- is the work function of the metal, and m is a constant. In our case, E_{PB} is taken as the Auger peak energy and is 60 eV for the Cu M_{23}VV and 40 eV for the Au O_{23}VV transitions. The Auger electron-induced extrinsic spectrum (Fig. 7) has been normalized such that

$$\int_0^{E_0} I_{\mathrm{LET}}^{\mathrm{extrinsic}}\, dE = I_{\mathrm{peak}}\{\delta_{\mathrm{surface}}[(1-T)/(T+R)] + \delta_{\mathrm{bulk}}[(1-R)/(T+R)]\}, \qquad (6)$$

where E_0 represents the upper limit of LET [50 (30) eV for Cu (Au)].

Integrating both sides of Eq. (2) and rearranging,

$$\int_0^{E_0} I_{\mathrm{LET}}^{\mathrm{intrinsic}}\, dE = \int_0^{E_0} I_{\mathrm{LET}}\, dE - \int_0^{E_0} I_{\mathrm{LET}}^{\mathrm{extrinsic}}\, dE, \qquad (7)$$

where E_0 has been defined earlier. Representing the integrated terms by the respective intensity terms [$\int I(E)dE \rightarrow I$] and dividing both sides by I_{peak},

$$I_{\mathrm{LET}}^{\mathrm{intrinsic}}/I_{\mathrm{peak}} = I_{\mathrm{LET}}/I_{\mathrm{peak}} - \delta_{\mathrm{surface}}[(1-T)/(T+R)] - \delta_{\mathrm{bulk}}[(1-R)/(T+R)]. \qquad (8)$$

Substituting the values for Cu (Au), $I_{\mathrm{LET}}/I_{\mathrm{peak}} = 3.73$ (3.4), $\delta_{\mathrm{bulk}} = 0.46$ (0.21),[19] $\delta_{\mathrm{surface}} = 1$, $T = 0.46$ (0.47), and $R = 0.05$, the ratio of the intrinsic part of the LET to the Auger peak area ($I_{\mathrm{LET}}^{\mathrm{intrinsic}}/I_{\mathrm{peak}}$) for Cu (Au) is 1.81 (2.0).

The Cu M_{23}VV and Au O_{23}VV Auger transitions with the estimated extrinsic contributions subtracted are shown in Fig. 8. The ratio of spectral weight in the intrinsic LET region to the main Auger peak is 1 : 1.81 (2.0) for Cu (Au). The intrinsic LET can be interpreted as due to core holes decaying via multielectron emission processes, e.g., a C-VVV process[1] in which two electrons are emitted. Other possible mechanisms for multielectron emission could include processes mediated by the plasmon generation and decay.[34] It would be interesting to theoretically explore the effect on the LET by collective excitations of the electron gas generated as a result of the creation of the core hole through the annihilation process.

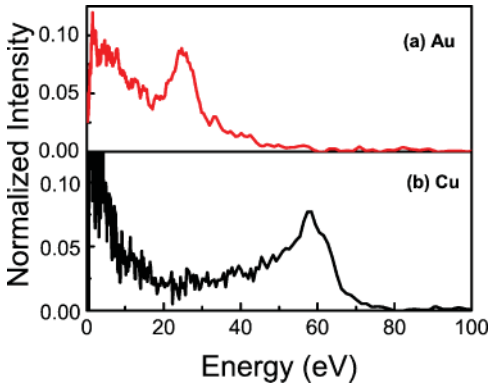

FIG. 8. (Color online) CVV Auger spectra of (a) Au and (b) Cu after the subtraction of the extrinsic contribution. The intrinsic LET due to C-VVV transitions extends to 0 eV and is ∼1.81 (2.0) times as intense as the Auger peak (CVV transition) for Cu (Au).

The spectra in Fig. 8 have been used to estimate the probability of core holes decaying via the proposed C-VVV process. Since such a process entails emission of two electrons (sharing the energy of the usual Auger electron), the spectral weight of the C-VVV process will be twice that of the conventional CVV process. Hence the percentage of core holes decaying via multielectron emission for Cu (Au) has been calculated to be ∼47 (50)%. The C-VVV emission probability has also been used to calculate the positron-core electron annihilation probability at surfaces. Earlier estimates[8] of the annihilation of surface-state positrons from PAES data considered only the core holes which decayed via the CVV process. The results of this study suggest the importance of C-VVV processes in estimating the number of initial core holes. Previous analysis (considering only CVV processes and inelastic scattering) resulted in estimates of 3.1% and 3% core-annihilation probability for Cu ($3p$) and Au ($5p$). Based on analysis using the full spectrum including the LET down to 0 eV, we find the core-annihilation probabilities would be 5.9% for Cu ($3p$) and 6% for Au ($5p$). The new estimate for Cu is in better agreement with the calculations of 6.9% (Ref. 35) and 9.2%.[36]

IV. CONCLUSION

We have reported background-free measurement of the complete spectra of low-energy electrons emitted as a result of Auger transition in metals. By depositing low-energy (∼1.5 eV) positrons directly into the surface state,[9] it was possible to excite Auger transitions from atoms at the surface without generating any primary-beam-induced secondary electrons. Localization of the positrons in the surface state ensures that almost all of the Auger transitions occur in the topmost atomic layer. The resultant spectra showed that the majority of the spectral weight is in the low-energy tail associated with the Auger peak and extends to 0 eV.

Our results suggest that the intrinsic part of the LET is due to a process in which the core hole decays by emission of more than one Auger electron (C-VVV). Assuming that the intrinsic process involves emission of only two electrons, it has been calculated that 47 (50)% of the core holes in Cu (Au) decay via multielectron emission. This result was used to

obtain a new estimate of the positron-core electron annihilation probability for Cu and Au which agree well with theoretical calculations. Since in the case of multielectron Auger emission the valence electrons are emitted simultaneously, our studies are analogous to spectroscopy of photon-induced emission of electron pairs[15] and provide another way of probing electron correlation effects in valence bands of metals.

Our results also have implications in quantitative analysis of Auger spectra.[37] In particular, we show that a significant fraction of low-energy core holes (<100 eV) in Cu and Au decay via multiple electron processes. These processes result in a decrease in the Auger peak intensity that is not fully accounted for by the background removal technique as suggested by Tougaard[4,38] or by reflection-electron-energy-loss spectroscopy-based background-subtraction scheme.[39] Consequently, estimates based upon measuring of the integrated intensity in the Auger peak region alone may lead to an underestimate of the number of initial core-hole excitations. This has important implications for the use of PAES in estimating positron-core electron annihilation probabilities[35] and for the use of Auger spectroscopy in the quantitative analysis of surfaces.

ACKNOWLEDGMENTS

We wish to acknowledge useful discussions with D. E. Ramaker, A.P. Mills, Jr., J. Moxom, and A.G. Hathaway. Useful suggestions by the referees are gratefully acknowledged. This work was supported by the Welch Foundation, Y1100 and NSF Grant No. DMR-0907679.

[1] D. E. Ramaker, J. Vac. Sci. Technol. A **7**, 1614 (1989).
[2] W. S. M. Werner, W. Smekal, H. Störi, H. Winter, G. Stefani, A. Ruocco, F. Offi, R. Gotter, A. Morgante, and F. Tommasini, Phys. Rev. Lett. **94**, 038302 (2005).
[3] M. I. Trioni, S. Caravati, G. P. Brivio, L. Floreano, F. Bruno, and A. Morgante, Phys. Rev. Lett. **93**, 206802 (2004).
[4] S. Tougaard, Surf. Interface Anal. **11**, 453 (1988).
[5] M. P. Seah, Surf. Sci. **32**, 703 (1972).
[6] ASTM standard E995-04, (ASTM International, West Conshohocken, PA, 2003) [http://www.astm.org/Standards/E995.htm].
[7] A. Weiss, R. Mayer, M. Jibaly, C. Lei, D. Mehl, and K. G. Lynn, Phys. Rev. Lett. **61**, 2245 (1988).
[8] K. O. Jensen and A. Weiss, Phys. Rev. B **41**, 3928 (1990).
[9] S. Mukherjee, M. P. Nadesalingam, P. Guagliardo, A. D. Sergeant, B. Barbiellini, J. F. Williams, N. G. Fazleev, and A. H. Weiss, Phys. Rev. Lett. **104**, 247403 (2010).
[10] E. Jensen, R. A. Bartynski, R. F. Garrett, S. L. Hulbert, E. D. Johnson, and C.-C. Kao, Phys. Rev. B **45**, 13636 (1992).
[11] C. P. Lund, S. M. Thurgate, and A. B. Wedding, Phys. Rev. B **49**, 11352 (1994).
[12] G. V. Riessen, Z. Wei, R. S. Dhaka, C. Winkler, F. O. Schumann, and J. Kirschner, J. Phys.: Condens. Matter **22**, 092201 (2010).
[13] H. Zhou, Ph.D. thesis, University of Texas at Arlington, 1996.
[14] T. A. Carlson and M. O. Krause, Phys. Rev. Lett. **14**, 390 (1965).
[15] N. Fominykh, J. Berakdar, J. Henk, and P. Bruno, Phys. Rev. Lett. **89**, 086402 (2002).
[16] S. Xie, Ph.D. thesis, University of Texas at Arlington, 2002.
[17] P. Kruit and F. H. Read, J. Phys. E **16**, 313 (1983).
[18] M. P. Nadesalingam, S. Mukherjee, S. Somasundaram, C. R. Chenthamarakshan Norma, R. de Tacconi, Krishnan Rajeshwar, and A. H. Weiss, Langmuir **23**, 1830 (2007).
[19] Y. Lin and D. C. Joy, Surf. Interface Anal. **37**, 895 (2005).
[20] C. Hugenschmidt, J. Mayer, and K. Schreckenbach, J. Phys.: Conf. Ser. **225**, 012015 (2010).
[21] E. N. Sickafus, Phys. Rev. B **16**, 1448 (1977).
[22] E. N. Sickafus, Phys. Rev. B **16**, 1436 (1977).
[23] W. Werner, H. Tratnik, J. Brenner, and H. Stori, Surf. Sci. **495**, 107 (2001).
[24] A. Knights and P. Coleman, Surf. Sci. **367**, 238 (1996); M. Farjam and H. B. Shore, Phys. Rev. B **36**, 5089 (1987).
[25] R. Mayer, A. Schwab, and A. Weiss, Phys. Rev. B **42**, 1881 (1990); E. Soininen, A. Schwab, and K. G. Lynn, *ibid*. **43**, 10051 (1991).
[26] Aleksander Jablonski, Phys. Rev. B **43**, 7546 (1991). Tabulated values are also maintained at [http://eaps4.iap.tuwien.ac.at/~werner/data_trc.html].
[27] D. Mehl, Ph.D. thesis, University of Texas at Arlington, 1990.
[28] D. Bote, F. Salvat, A. Jablonski, and C. J. Powell, J. Electron Spectrosc. Relat. Phenom. **175**, 41 (2009).
[29] A. Jablonski, I. S. Tilinin, and C. J. Powell, Phys. Rev. B **54**, 10927 (1996).
[30] M. P. Seah and I. S. Gilmore, Surf. Interface Anal. **31**, 835 (2001).
[31] C. J. Powell and A. Jablonski, NIST Electron Effective-Attenuation-Length Database, Version 1.3, SRD 82, National Institute of Standards and Technology, Gaithersburg, MD (2011).
[32] J. Mayer, C. Hugenschmidt, and K. Schreckenbach, Appl. Surf. Sci. **255**, 220 (2008).
[33] M. P. Seah, Surf. Sci. **17**, 132 (1969).
[34] W. S. M. Werner, A. Ruocco, F. Offi, S. Iacobucci, W. Smekal, H. Winter, and G. Stefani, Phys. Rev. B **78**, 233403 (2008).
[35] N. Fazleev, M. Nadesalingam, W. Maddox, S. Mukherjee, K. Rajeshwar, and A. Weiss, Surf. Sci. **604**, 32 (2010).
[36] M. Alatalo, B. Barbiellini, M. Hakala, H. Kauppinen, T. Korhonen, M. J. Puska, K. Saarinen, P. Hautojarvi, and R. M. Nieminen, Phys. Rev. B **54**, 2397 (1996).
[37] M. P. Seah, Surf. Interface Anal. **24**, 830 (1996).
[38] S. Tougaard, Surf. Sci. **182**, L253 (1987).
[39] M. P. Seah, I. S. Gilmore, and S. J. Spencer, Surf. Interface Anal. **31**, 778 (2001).